# Investigation of GaN Films Grown on Liquid-Phase Deposited SiO₂ Nanopatterned Sapphire Substrates

## Cheng-Yu Hsieh, Bo-Wen Lin, Hsin-Ju Cho, Bau-Ming Wang, and YewChung Sermon Wu*,z

*Department of Materials Science and Engineering, National Chiao Tung University, Hsinchu 300, Taiwan*

A simple, easy and relatively inexpensive liquid phase deposition (LPD) method was used to introduce nano SiO₂ on sapphire substrates to fabricate nanoscale patterned sapphire substrates (PSS). Two kinds of nanoscale PSS were used to grow GaN, namely "NPOS" which is nano-pattern oxide on sapphire substrate and "NPSS" which is nano-patterned sapphire substrate. It was found that upper region of NPSS-GaN had the best quality. This is because as the growth time increased, laterally-grown GaN caused the threading dislocations to bend toward the patterns. Besides, voids formed on the NPSS pattern sidewalls caused more threading dislocation bending toward these voids.

High-brightness GaN-based light-emitting diodes (LEDs) have been highly demanded in various fields. For the purpose of next-generation application of solid-state lighting, LEDs with higher internal and external quantum efficiency are required. Among many methods, lots of efforts have been invested on patterned sapphire substrates (PSS) to improve the quality of GaN film and light extraction efficiency.[1–3]

In PSS, microscale patterned substrates with grooves, pyramids or other patterns are usually fabricated by dry or wet etching process. As the growth time increased, GaN epilayers on the c-plane sapphire covered these patterns by lateral growth causing the threading dislocation to bend toward the microscale patterns. Therefore, the threading dislocation densities on the upper regions were reduced.[1] As a result, the internal quantum efficiency and the leakage current of GaN-based LEDs were improved.[4–6]

If the lateral overgrowth approach is reduced to the nanoscale, theoretical and experimental studies indicate that a further reduction in the defect density is possible.[7] Several technologies have been applied to fabricate nanoscale PSS like nanoimprint lithography, nanosphere lithography and forming nanorods by using self-assembled Ni as etching mask.[8–12] In this study, liquid phase deposition (LPD) was used to introduce nanoscale SiO₂ hemispheres on sapphire substrates to fabricate nanoscale PSS's.[12–15] Compared to other nanoscale PSS process, the LPD-SiO₂ process was simpler, easier and relatively inexpensive. With these nanoscale patterns, the crystal quality and optical performance of GaN were improved.

## Experimental

Two kinds of nanoscale PSS were used to grow GaN. Samples designated as "NPOS" are nano-pattern oxide on sapphire substrate, while samples designated as "NPSS" are nano-patterned sapphire substrate. Two-inch c-plane sapphire substrate was used in this study. LPD was used to fabricate NPOS. Sapphire substrate was first immersed in mixed solution of $H_2SiF_6$ saturated with silica gel and $H_3BO_3$ (0.01 mol/l) for 60 min. The related LPD reaction equations on sapphire substrate were listed as follows:

$$H_3BO_3 + 4HF \leftrightarrow BF_4^- + H_3O^+ + 2H_2O \tag{1}$$

$$H_2SiF_6 + 2H_2O \leftrightarrow 6HF + SiO_2 \tag{2}$$
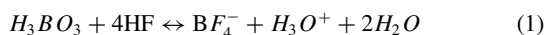
$SiO_2$ can be formed after the dehydration of OH-bonded siloxane oligomer $[SiF_m(OH)_{4-m}]$ by catalytic reaction.[12] These substrates were then annealed at 900°C in $N_2$ ambient for 30 minutes to improve $SiO_2$ quality.

To fabricate the NPSS, NPOS was etched in hot $H_3PO_4$–based solutions. Then, samples were dipped into 1% diluted hydrogen fluoride (DHF) solution to remove the LPD- $SiO_2$.[16]

*Electrochemical Society Active Member.
zE-mail: SermonWu@StanfordAlumni.org

After the cleaning process, GaN-based LED structures were grown by metal-organic chemical vapor deposition (MOCVD) on both substrates. For the purpose of comparison, LED structures were also grown on unpatterned sapphire substrate and denoted as FLAT. The crystal quality and optical performance of GaN were characterized by atomic force microscopy (AFM), scanning electron microscopy (SEM), transmission electron-microscopy (TEM), X-ray diffraction (XRD), monochromated cathodoluminescence (CL) and photoluminescence (PL).

## Results and Discussion

Figure 1 presents the SEM images of NPOS and NPSS. The shape of LPD-SiO₂ patterns on the surface of sapphire was hemisphere with 200–300 nm in diameter and 100–150 nm in height (measured by AFM). As shown in Figs. 1a, these SiO₂ hemispheres were randomly distributed on the sapphire surface. The structure of NPSS pattern comprised a triangle pyramid covered with a flat top (0001) c-plane. The diameter of pyramids was about 250–300 nm, and the height was 140–170 nm.

The nature of GaN crystal qualities on sapphire substrates was first analyzed by XRD rocking curves. Both symmetric (002) and asymmetric (102) reflections were measured as shown in Table I. The full width at half maximum (FWHM) values of NPSS-GaN were less than those of NPOS-GaN and FLAT-GaN. These results indicate that the GaN crystallinity of NPSS-GaN is superior to that of NPOS-GaN and FLAT-GaN.

Figure 2 is cross section SEM images and corresponding monochromated CL maps taken at wavelengths of 370 nm, respectively. Clearly, the upper region of the GaN film exhibited bright contrast in the CL maps which correspond to strong excitation with much less non-radiative centers in this region. In contrast, the lower region appeared dark contrast, implying that it is highly defected. Besides, Fig. 2 also shows that the CL contrast of the upper regions of NPSS-GaN and NPOS-GaN was brighter than that of FLAT-GaN.

The CL spectra intensities collected around the lower and upper regions are summarized in Table I. At the lower regions, the integral intensities of NPSS-GaN and NPOS-GaN were about the same
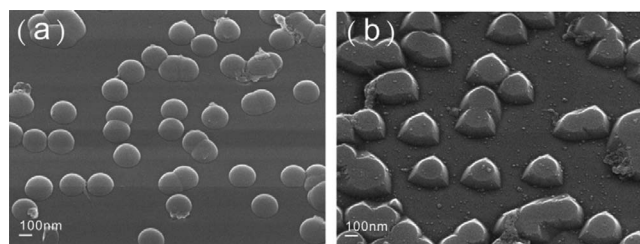


**Figure 1.** SEM images of (a) NPOS and (b) NPSS.

**Table I.  Characteristics of GaN grown on sapphire.**

| | FWHM of XRCs (arcsec) | | | Integral CL spectrum | |
|---|---|---|---|---|---|
| | (002) | (102) | EPD (cm$^{-2}$) | lower region | upper region |
| FLAT-GaN | 427.9 | 586.9 | $3.3 \times 10^7$ | $2.9 \times 10^4$ | $3 \times 10^5$ |
| NPOS-GaN | 389.2 | 522.9 | $8 \times 10^6$ | $9.3 \times 10^4$ | $1.5 \times 10^6$ |
| NPSS-GaN | 362.4 | 390.1 | $3.9 \times 10^6$ | $9.1 \times 10^4$ | $1.9 \times 10^6$ |

($\sim$9 $\times$ $10^4$), which was 3 times higher than that of FLAT-GaN. At the upper regions, the integral intensity of NPSS-GaN was $1.9 \times 10^6$, which was 1.27 times higher than that of NPOS-GaN, and 6.33 times higher than that of the FLAT-GaN.

The improvement on structural quality at the upper region was verified by measuring etch pit density (EPD). All three samples were grinded till undoped-GaN revealed ($\sim$2.5 $\mu$m from the GaN/sapphire interface). Then, the samples were etched in 270°C H$_3$PO$_4$ for 3 min. As listed in Table I, the EPD of NPSS-GaN was $3.9 \times 10^6$ cm$^{-2}$, which was 48.75% of NPOS-GaN, and 11.82% of FLAT-GaN. In other words, NPSS-GaN did have the best crystal quality at the upper region.

TEM was also used to investigate the crystal qualities in both regions. As shown in Fig. 3a, many dislocations were observed at the lower region. They originated from the GaN/sapphire interface due to the large lattice misfit. Many of them then extended to the upper region. As for the NPSS-GaN and NPOS-GaN (Figs. 3b and 3c), as the growth time increased, GaN epilayers on the c-plane sapphire covered these nano patterns by lateral growth causing the threading dislocation to bend toward the patterns. Therefore, the dislocation densities on the upper regions were reduced.

These TEM observations clearly explain the CL observations. That the upper regions of the GaN film exhibited bright CL contrasts is because these regions had low defect/dislocation densities. Besides, that the CL contrast of the upper regions of NPSS-GaN and NPOS-GaN was brighter than that of FLAT-GaN is because their threading dislocation bended toward the nano patterns at the lower regions. As a result, their upper regions had low defect densities.

Figures 3b and 3c also reveal that NPSS-GaN patterns had more bending dislocations than NPOS-GaN at the lower regions. This might be because the GaN growth mechanism on NPSS was different from that on NPOS. As illustrated in Fig. 4a, most of the growth of GaN on NPOS was initiated from bottom c-planes. As the growth time increased, lateral growth GaN epilayers caused the threading dislocations to bend toward the patterns, as mentioned previously.[1]

As illustrated in Fig. 4d, GaN initiates not only from bottom c-planes, but also from top c-planes for the growth of NPSS-GaN. It is evident that as the growth time increased, the two growth fronts collided to each other. As a result, some voids ($\sim$50 nm in size) were left on the pattern sidewall, as shown in Figs. 3c and 4b. These voids were associated with the relaxed morphologies of the GaN film side faces and caused more threading dislocation to bend toward these voids. Consequently, the threading dislocation density was effectively reduced.[17]

PL was used to investigate the quality of muti-quantum wells. The excitation source was a 325 nm, 30 mW He–Cd continuous wave laser. As Fig. 5 shows, the PL peak intensity of MQWs grown on NPSS is 1.2 times higher than that on NPOS, and 1.5 times higher than that on FLAT. This observation suggests that nano patterns in NPSS can efficiently improve MQWs quality via improving crystal quality at the upper region (through bending threading dislocations toward the patterns at the lower regions).
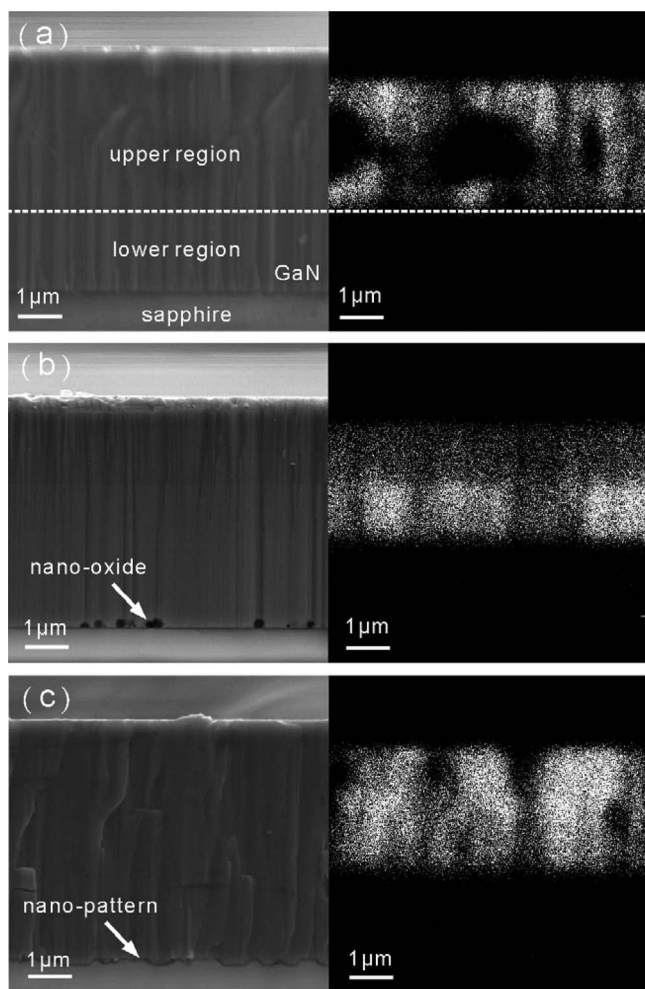


**Figure 2.** SEM images and corresponding monochromated CL maps of (a) FLAT-GaN, (b) NPOS -GaN and (c) NPSS -GaN.
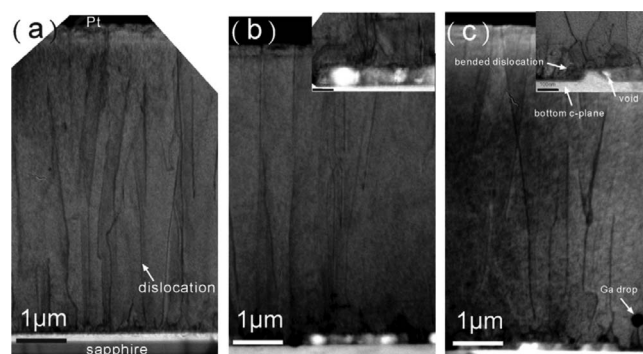


**Figure 3.** Cross-section TEM images of GaN grown on (a) FLAT sapphire, (b) NPOS, and (c) NPOS. The black dots in image are Ga drops formed from FIB ion milling.
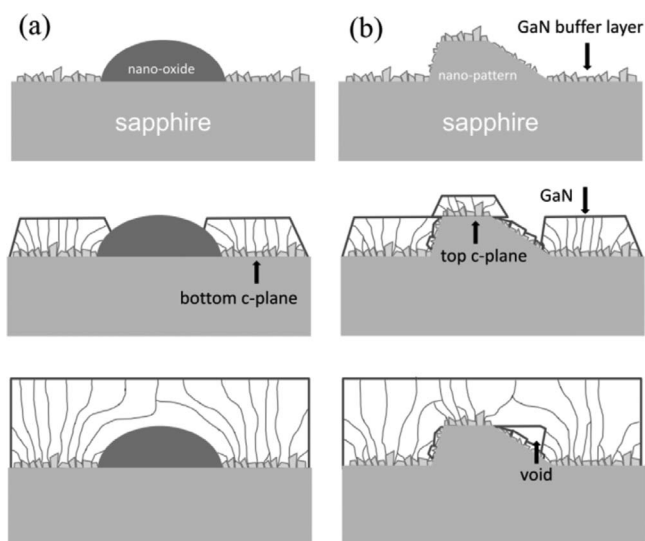
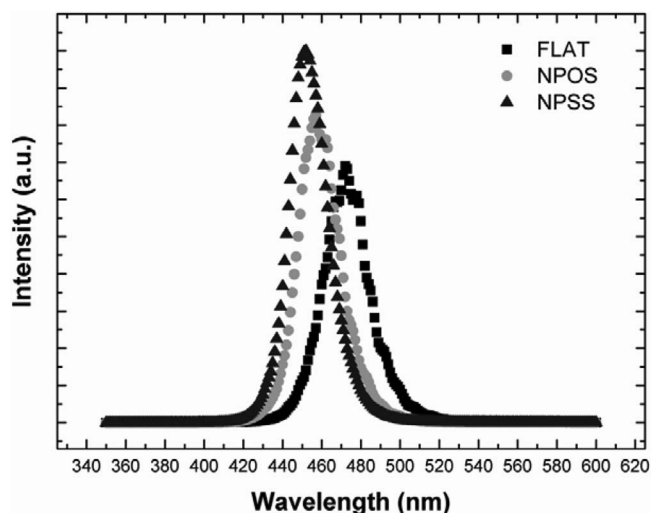**Figure 4.** Schematic diagrams of evolution of GaN grown on (a) NPOS and (b) NPOS.



**Figure 5.** The photoluminescence of muti-quantum-wells grown on FLAT sapphire, NPOS and NPSS.

## Conclusions

High quality $SiO_2$ hemispheres and sapphire nano-patterns are fabricated on sapphire substrate by combining LPD method and wet etch process. The GaN films have fully coalesced and the voids can only be found in the case of GaN grown on NPSS. The XRCs, EPD and monochromated CL maps show that the GaN grown on PSSs has better quality than on FLAT sapphire. Moreover, the integral CL spectra show that the GaN grown on NPSS has relatively lower defect density than on NPOS and FLAT sapphire. TEM analysis reveal that parts of dislocation in the GaN grown on NPSS bend to voids and hence largely lower the defect density. The MQWs grown on NPOS and NPSS indicate 1.2 and 1.5 times enhancement in PL intensity than that in FLAT sapphire.

## References

1. J. H. Cheng, Y. C. Sermon Wu, W. C. Liao, and B. W. Lin, *Appl. Phys. Lett.*, **96**, 051109 (2010).
2. B. W. Lin, C. Y. Hsieh, B. M. Wang, W. C. Hsu, and Y. C. Sermon Wu, *Electrochem. Solid-State Lett.*, **14**, 48 (2011).
3. B. W. Lin, C. C. Chang, C. Y. Hsieh, B. M. Wang, Y. C. Sermon Wu, and W. C. Hsu, *IEEE Photon. Tech. Lett.*, **23**, 1772 (2011).
4. I. Lo, K. Y. Hsieh, S. L. Hwang, and L. W. Tu, *Appl. Phys. Lett.*, **74**, 2167 (1999).
5. P. Kozodoy, J. P. Ibbetson, H. Marchand, P. T. Fini, S. Keller, J. S. Speck, S. P. DenBaars, and U. K. Mishra, *Appl. Phys. Lett.*, **73**, 17 (1998).
6. K. Tadatomo, H. Okagawa, Y. Ohuchi, T. Tsunekawa, Y. Imada, M. KaTo, and T. Taguchi, *Jpn. J. Appl. Phys.*, **40**, L583 (2001).
7. H. Gao, F. Yan, Y. Zhang, J. Li, Y. Zeng, and G. Wang, *J. Appl. Phys.*, **103**, 014314 (2008).
8. S. Y. Chou, P. R. Krauss, and P. J. Renstrom, *J. Vac. Sci. Technol. B*, **14**, 4129 (1996).
9. H. W. Huang, C. H. Lin, J. K. Huang, K. Y. Lee, C. F. Lin, C. C. Yu, J. Y. Tsai, R. Hsueh, H. C. Kuo, and S. C. Wang, *Mater. Sci. Eng. B*, **164**, 76 (2009).
10. C. H. Chiu, H. H. Yen, C. L. Chao, Z. Y. Li, and P. Yu, *Appl. Phys. Lett.*, **93**, 081108 (2008).
11. J. J. Chen, Y. K. Su, C. L. Lin, S. M. Chen, W. L. Li, and C. C. Kao, *IEEE Photon. Tech. Lett.*, **20**, 1193 (2008).
12. C. H. Chan, C. H. Hou, S. Z. Tseng, T. J. Chen, and H. T. Chien, *Appl. Phys. Lett.*, **95**, 011110 (2009).
13. H. Nagayama, H. Honda, and H. Kawahara, *J. Electrochem. Soc.*, **138**, 2013 (1988).
14. M. C. Hsu, Y. M. Sun, I. C. Leu, and M. H. Hon, *J. Electrochem. Soc.*, **153**, F260 (2006).
15. M. K. Lee, C. L. Ho, and C. H. Fan, *Appl. Phys. Lett.*, **92**, 061103 (2008).
16. F. Dwikusuma, D. Saulys, and T. F. Kuech, *J. Electrochem. Soc.*, **149**, G603 (2002).
17. W. K. Wang, D. S. Wuu, W. C. Shih, J. S. Fang, W. Y. Lin, P. Han, R. H. Horng, T. C. Hsu, T. C. Huo, M. J. Jou, A. Lin, and Y. H. Yu, *Jpn. J. Appl. Phys.*, **44**, 2512 (2005).